Towards total photonic control of complex-shaped colloids by vortex beams

Clayton P. Lapointe,[1,2] Thomas G. Mason,[2,4] and Ivan I. Smalyukh[1,3,5]

[1]*Department of Physics and Liquid Crystals Materials Research Center, University of Colorado at Boulder, Boulder, CO 30309, USA*

[2]*Department of Physics and Astronomy, Department of Chemistry and Biochemistry, and California NanoSystems Institute, University of California at Los Angeles, Los Angeles, CA 90095, USA*

[3]*Renewable and Sustainable Energy Institute, University of Colorado and National Renewable Energy Laboratory, Boulder, CO 30309, USA*

[4]*mason@physics.ucla.edu*

[5]*ivan.smalyukh@colorado.edu*

Abstract: We demonstrate optical trapping and orientational control over colloidal particles having complex shapes in an anisotropic host fluid using a dynamic holographic optical tweezers system. Interactions between a colloidal particle and the toroidal intensity distributions of focused Laguerre-Gaussian beams allow for stable optical tweezing and provide a tunable tilt of the particle out of the focal plane. Use of an aligned nematic liquid crystal as the host fluid suppresses rotations about the optical axis arising from angular momentum transfer from the beam and effectively defines a rotational axis for the colloid within the trap.

OCIS codes: (140.7010) Laser trapping; (160.3710) Liquid crystals; (350.4855) Optical tweezers or optical manipulation.

References and links

1. A. Ashkin, J. M. Dziedzic, J. E. Bjorkholm, and S. Chu, "Observation of a single-beam gradient force optical trap for dielectric particles," Opt. Lett. **11**(5), 288–290 (1986).
2. S. M. Block, L. S. B. Goldstein, and B. J. Schnapp, "Bead movement by single kinesin molecules studied with optical tweezers," Nature **348**(6299), 348–352 (1990).
3. J. C. Crocker and D. G. Grier, "Microscopic measurement of the pair interaction potential of charge-stabilized colloid," Phys. Rev. Lett. **73**(2), 352–355 (1994).
4. D. G. Grier, "A revolution in optical manipulation," Nature **424**(6950), 810–816 (2003).
5. M. E. J. Friese, T. A. Nieminen, N. R. Heckenberg, and H. Rubinsztein-Dunlop, "Optical alignment and spinning of laser-trapped microscopic particles," Nature **394**(6691), 348–350 (1998).
6. Z. Cheng, P. M. Chaikin, and T. G. Mason, "Light streak tracking of optically trapped thin microdisks," Phys. Rev. Lett. **89**(10), 108303 (2002).
7. J. N. Wilking and T. G. Mason, "Multiple trapped states and angular Kramers hopping of complex dielectric shapes in a simple optical trap," Europhys. Lett. **81**(5), 58005 (2008).
8. T. Asavei, V. L. Y. Loke, M. Barbieri, T. A. Nieminen, N. R. Heckenberg, and H. Rubinsztein-Dunlop, "Optical angular momentum transfer to microrotors fabricated by two-photon photopolymerization," N. J. Phys. **11**(9), 093021 (2009).
9. P. Galajda and P. Ormos, "Orientation of flat particles in optical tweezers by linearly polarized light," Opt. Express **11**(5), 446–451 (2003).
10. S. L. Neale, M. P. MacDonald, K. Dholakia, and T. F. Krauss, "All-optical control of microfluidic components using form birefringence," Nat. Mater. **4**(7), 530–533 (2005).
11. J. E. Curtis and D. G. Grier, "Structure of optical vortices," Phys. Rev. Lett. **90**(13), 133901 (2003).
12. J. E. Curtis and D. G. Grier, "Modulated optical vortices," Opt. Lett. **28**(11), 872–874 (2003).
13. V. Bingelyte, J. Leach, J. Courtial, and M. J. Padgett, "Optically controlled three-dimensional rotation of microscopic objects," Appl. Phys. Lett. **82**(5), 829–831 (2003).
14. M. Yada, J. Yamamoto, and H. Yokoyama, "Direct observation of anisotropic interparticle forces in nematic colloids with optical tweezers," Phys. Rev. Lett. **92**(18), 185501 (2004).
15. I. I. Smalyukh, O. D. Lavrentovich, A. N. Kuzmin, A. V. Kachynski, and P. N. Prasad, "Elasticity-mediated self-organization and colloidal interactions of solid spheres with tangential anchoring in a nematic liquid crystal," Phys. Rev. Lett. **95**(15), 157801 (2005).
16. R. P. Trivedi, D. Engström, and I. I. Smalyukh, "Optical manipulation of colloids and defect structures in anisotropic liquid crystal fluids," J. Opt. **13**(4), 044001 (2011).

#148001 - $15.00 USD Received 23 May 2011; revised 14 Jul 2011; accepted 10 Aug 2011; published 1 Sep 2011

17. D. Engström, R. P. Trivedi, M. Persson, M. Goksör, K. A. Bertness, and I. I. Smalyukh, "Three-dimensional imaging of liquid crystal structures and defects by means of holographic manipulation of colloidal nanowires with faceted sidewalls," Soft Matter **7**(13), 6304–6312 (2011).
18. C. P. Lapointe, T. G. Mason, and I. I. Smalyukh, "Shape-controlled colloidal interactions in nematic liquid crystals," Science **326**(5956), 1083–1086 (2009).
19. F. Mondiot, S. P. Chandran, O. Mondain-Monval, and J.-C. Loudet, "Shape-induced dispersion of colloids in anisotropic fluids," Phys. Rev. Lett. **103**(23), 238303 (2009).
20. F. R. Hung, O. Guzmán, B. T. Gettelfinger, N. L. Abbott, and J. J. de Pablo, "Anisotropic nanoparticles immersed in a nematic liquid crystal: defect structures and potentials of mean force," Phys. Rev. E Stat. Nonlin. Soft Matter Phys. **74**(1), 011711 (2006).
21. M. Škarabot, M. Ravnik, D. Babic, N. Osterman, I. Poberaj, S. Zumer, I. Musevic, A. Nych, U. Ognysta, and V. Nazarenko, "Laser trapping of low refractive index colloids in a nematic liquid crystal," Phys. Rev. E Stat. Nonlin. Soft Matter Phys. **73**(2), 021705 (2006).
22. I. I. Smalyukh, A. V. Kachynski, A. N. Kuzmin, and P. N. Prasad, "Laser trapping in anisotropic fluids and polarization-controlled particle dynamics," Proc. Natl. Acad. Sci. U.S.A. **103**(48), 18048–18053 (2006).
23. H. F. Gleeson, T. A. Wood, and M. Dickinson, "Laser manipulation in liquid crystals: an approach to microfluidics and micromachines," Philos. Transact. A Math. Phys. Eng. Sci. **364**(1847), 2789–2805 (2006).
24. C. P. Lapointe, S. Hopkins, T. G. Mason, and I. I. Smalyukh, "Electrically driven multiaxis rotational dynamics of colloidal platelets in nematic liquid crystals," Phys. Rev. Lett. **105**(17), 178301 (2010).
25. E. R. Dufresne and D. G. Grier, "Optical tweezer arrays and optical substrates created with diffractive optics," Rev. Sci. Instrum. **69**(5), 1974–1977 (1998).
26. J. E. Curtis, B. A. Koss, and D. G. Grier, "Dynamic holographic optical tweezers," Opt. Commun. **207**(1-6), 169–175 (2002).
27. C. J. Hernandez and T. G. Mason, "Colloidal alphabet soup: monodisperse dispersions of shape-designed lithoparticles," J. Phys. Chem. C **111**(12), 4477–4480 (2007).
28. S. D. Durbin, S. M. Arakelian, and Y. R. Shen, "Optical-field-induced birefringence and Freedericksz transition in a nematic liquid crystal," Phys. Rev. Lett. **47**(19), 1411–1414 (1981).
29. M. A. Clifford, J. Arlt, J. Courtial, and K. Dholakia, "High-order Laguerre–Gaussian laser modes for studies of cold atoms," Opt. Commun. **156**(4-6), 300–306 (1998).
30. D. McGloin, G. C. Spalding, H. Melville, W. Sibbett, and K. Dholakia, "Three-dimensional arrays of optical bottle beams," Opt. Commun. **225**(4-6), 215–222 (2003).
31. R. Agarwal, K. Ladavac, Y. Roichman, G. Yu, C. M. Lieber, and D. G. Grier, "Manipulation and assembly of nanowires with holographic optical traps," Opt. Express **13**(22), 8906–8912 (2005).

1. Introduction

Laser tweezers [1] have provided an unprecedented level of control over fluid-borne particles, leading to experiments that have probed the intricate stepping of molecular motors [2], interparticle interactions [3], and colloidal assembly [4]. Using laser tweezers to manipulate non-spherical colloids is highly valuable, yet orientational control is currently limited. For example, by controlling the polarization state of the beam, birefringent and shape anisotropic particles can be rotated and oriented [5–10], however, only around the optical axis of the trapping beam. Laser tweezers based on Laguerre-Gaussian (LG) modes or optical vortices [11,12], carry angular momentum that can apply torques to colloids, yet these still only induce rotations about the beam axis. Stable 3D orientational control has been demonstrated for a specific class of colloidal shapes containing at least two spherical segments that can be independently optically trapped using two Gaussian optical traps [13]. Here, we demonstrate that dielectric colloids having complex shapes, such as triangular and square-shaped platelets, suspended in an aligned nematic liquid crystal (NLC) can be stably trapped, oriented, and rotated about a predetermined axis that is orthogonal to the trapping laser beam's axis. We achieve this using a single Laguerre-Gaussian laser beam holographically generated by means of a spatial light modulator. The elasticity of the NLC suppresses particle rotations about the beam axis and provides a unique and controlled rotational axis within the focal plane.

In conventional implementations of single beam optical tweezers, a tightly focused laser beam generates optical gradient forces that can hold nanometer- and micrometer-scale colloids within a three dimensional optical trap. Stable traps require that the gradient forces are larger than scattering forces arising from radiation pressure and that the depth of the optical potential well is significantly larger than thermal energy $k_B T$ so that the colloid cannot escape the trap via diffusive motion. Although a multitude of non-spherical colloidal shapes such as disks [6], rotors [8], gears [10], and other complex shapes [7] have been trapped and manipulated with optical tweezers, the degree of orientational control is usually limited to a

#148001 - $15.00 USD Received 23 May 2011; revised 14 Jul 2011; accepted 10 Aug 2011; published 1 Sep 2011

single fixed orientation of the particle relative to the laser propagation direction, and in some cases the direction of polarization [6,7,9]. Furthermore, optical tweezing of spherical colloids suspended in NLCs has been extensively studied allowing for quantitative measurements of their interactions [14,15–17,20–22] and hydrodynamic drag [23].

The anisotropic elasticity of NLCs can orient and levitate non-spherical colloids, which can be controlled via particle shape [18] or external fields [24]. NLCs are composed of rod-shaped molecules that spontaneously align in the nematic phase with their long-axes parallel while their centers of masses are disordered. The director **n**, a unit-vector with inversion symmetry (**n** ≡ **-n** since NLCs lack polar order), represents the spatially varying average alignment direction of the molecules. Deforming **n** away from a uniform state through either surface interactions or external fields costs elastic energy. Micron-scale colloidal particles suspended in a NLC induce elastic deformations of **n** due to the anchoring of the NLC on the surface of the particles. These distortions can mediate anisotropic interactions between pairs of colloids [14–18] as well as energetically preferential orientations of non-spherical colloids [18–20] relative to the far-field director $\mathbf{n}_0$.

The equilibrium orientations are highly dependent upon particle shape and are dictated by minimizing the elastic energy associated with director deformations consistent with strong anchoring of **n** tangential to the colloids' surfaces [18]. In a uniformly aligned NLC, triangular particles align with one side parallel to $\mathbf{n}_0$ whereas squares align with one diagonal axis along $\mathbf{n}_0$, as shown in the micrographs under crossed polarizers in Fig. 1. Due to their plate-like shape and the planar anchoring on the bounding walls, both shapes orient with their larger-area faces lying parallel to the bounding walls. Elastic repulsion between the particles and the bounding substrates provides a levitating force that overcomes gravity and suspends them in the NLC bulk, allowing for controlled holographic optical tweezing [25,26] experiments using colloids suspended away from both the top and bottom walls.

2. Sample preparation

Custom-designed platelet colloidal particles are fabricated on Si wafers out of SU-8 photoresist using an i-line reduction stepper (Ultratech XLS) [27]. For these studies, we prepared 1 μm thick triangular and square-shaped colloids having edge lengths of 3.0 μm and 4.5 μm, respectively. The squares have a centered, square hole having 2 μm sides. After fabrication, the particles are dispersed at low volume fraction ($\phi \sim 10^{-4}$) in the room temperature nematic liquid crystal pentylcyanobiphenyl (5CB) [18]. Sample cells are assembled using glass slides that are coated with a thin layer of cured polyimide (PI 2555, HD Microsystems). The polyimide films are unidirectionally rubbed using fine pile velour to define the anchoring easy-axis (i.e. the direction that the long-axes of the NLC molecules preferentially align at the surface). The rubbing direction on the top and bottom inner alignment layers of the cell are oriented parallel so that alignment direction of the NLC throughout the cell is uniform and parallel to the rubbing. The thickness of the gap between the two glass slides is defined using 10 μm diameter glass bead spacers.

SU-8 possesses an index of refraction ($n \approx 1.6$) intermediate between the extraordinary and ordinary refractive indices of 5CB, $n_{\parallel} \approx 1.7$ and $n_{\perp} \approx 1.5$, respectively. To facilitate stable trapping of SU-8 colloids in 5CB, we polarize the beam of the optical tweezers perpendicular to $\mathbf{n}_0$, so that the effective refractive index of the surrounding fluid, $n_{\text{eff}} = n_{\perp} \approx 1.5$, is lower than that of the particle. We keep the laser power ≤ 20 mW to avoid optically induced re-alignment of the NLC [28], which for 5CB has a threshold power of ≈30 mW for a TEM_{00} mode optical trap at 1064 nm [21]. At these powers, no significant heating of the colloids or 5CB due to optical absorption is observed.

#148001 - $15.00 USD Received 23 May 2011; revised 14 Jul 2011; accepted 10 Aug 2011; published 1 Sep 2011

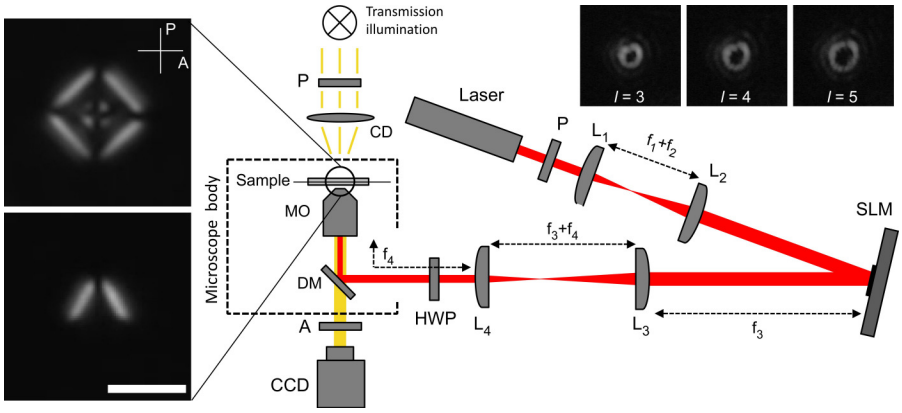

Fig. 1. Schematic of dynamic holographic optical tweezers. The output beam (red) from a ytterbium-doped fiber laser is expanded with a telescope (L_1 and L_2) to overfill the pixel array of a reflective spatial light modulator (SLM). The reflected beam size is reduced with a second telescope (L_3 and L_4) to fill the back aperture of a microscope objective (MO). A rotatable halfwave plate (HWP) controls the linear polarization state of the beam and the dichroic mirror (DM) is used to direct the beam into MO while allowing visible light (yellow) transmitted through the sample to travel to the CCD camera. A polarizer (P) located before the condenser (CD) and an analyzer (A) mounted below the sample allow for observations under crossed polarizers such as the images of a square colloid (top) and a triangular colloid (bottom) in 5CB shown on the left (scale bar: 5 μm). The SLM is capable of generating Laguerre-Gaussian optical vortices as shown in the images of the intensity distributions within the focal plane; charges l = 3, 4, 5 (left to right) in the top right.

3. Dynamic holographic optical tweezers

Phase profiles are imprinted on the wavefront of a collimated beam from a continuous wave ytterbium-doped fiber laser (IPG Photonics, λ = 1064 nm) using an electronically addressed, reflective SLM (P512-1064, Boulder Nonlinear Systems). The SLM is operated in a phase-only mode which controls the phase of the reflected wavefront from 0 to 2π radians pixel by pixel with a spatial resolution limited by the SLM's pixel size (15 μm x 15 μm). A telescope comprised of two plano-convex lenses is used to expand the 5 mm diameter beam output from the laser to overfill the 512x512 pixel array of the SLM and a second telescope reduces the reflected beam size to fill the back aperture of a high numerical aperture, infinity corrected 100x oil-immersion objective (Olympus UPLSAPO-100XO). The objective is corrected for chromatic aberrations up to the infrared, which assures that the imaging focal plane at visible wavelengths coincides with the image plane of the optical tweezers to ≈0.3 μm. A beam steerer and a dichroic mirror (Chroma) mounted within the fluorescence cube turret of an inverted, laser-scanning confocal microscope (Olympus IX-81 FV300) are used to align and direct the beam into the microscope objective. The linear polarization state of the beam is controlled using a rotatable halfwave plate. Brightfield images are acquired with a CCD video camera. Commercially available software (HOTgui, Arryx Inc.) is used to calculate holograms in real time and relay them to the spatial light modulator with a refresh rate of 15 Hz. The software is capable of generating multiple optical traps at user-defined locations within the field of view with a spatial accuracy of one camera pixel (≈50 nm). For each trap, a LG charge l can be specified which transforms the beam mode from a Gaussian TEM_{00} (l = 0) to an LG optical vortex giving rise to a toroidal intensity distribution within the focal plane (inset of Fig. 1). The radius of the vortex increases linearly with increasing l and the extent of the intensity distribution out of the focal plane decreases with increasing l. The intensity along the circumference of the vortex is modulated due to the pixilated nature of the phase profile generated by the SLM [11,12].

#148001 - $15.00 USD Received 23 May 2011; revised 14 Jul 2011; accepted 10 Aug 2011; published 1 Sep 2011

4. Results and discussion

In our experiments, the light sculpting capabilities of dynamic holographic optical tweezers [25] are utilized to produce and steer optical vortex traps, and video microscopy is used to determine the orientation, position, and stability of isolated colloids within focused optical vortex beams as a function of charge. Platelet colloids initially lying with their long-axes parallel to the focal plane and brought near the focus of a TEM_{00} mode optical trap are pulled into the high intensity region of the trap and rotate to an upright orientation. This orientation maximizes the volume of the high-index colloid within the most intense region of the optical trap. In the nematic phase, this rotational response is constrained to occur about $\mathbf{n}_0$ [18], precluding rotations about the beam axis arising from the optical momentum transfer from the beam to the colloid [8]. Changing the beam mode to an appropriately sized optical vortex with $l \neq 0$ such that the ring-like intensity distribution matches the volume of the colloid allows for stable optical tweezing of certain plate-like colloids with their long-axes parallel to the focal plane.

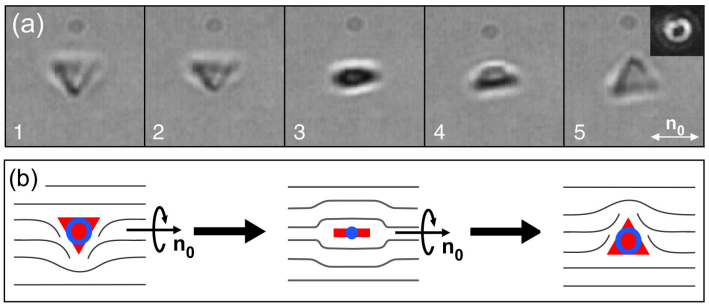

Fig. 2. (a) A series of video frames (Media 1) showing that a triangle initially held in an optical vortex with $l = 3$ (inset), rotates ≈90° to an upright orientation after switching the beam mode to $l = 0$. After the beam mode is switched back to $l = 3$, the triangle responds with another ≈90° rotation. (b) Schematic drawings showing the nematic director **n** (gray curves) in the vicinity of the triangle and the high intensity regions (blue) of the optical vortex for $l = 3$ and $l = 0$.

Dynamic switching of the optical vortex's charge allows for controlled rotations out of the focal plane. For example, in response to changing the beam mode from $l = 3$ to $l = 0$, a triangular colloid rotates 90° about $\mathbf{n}_0$ to an upright orientation without any accompanying translation as can be seen in the series of video frames in Fig. 2 (Media 1). Switching the beam mode back to $l = 3$ results in a further 90° rotation so that the triangle is once again trapped in-plane within the high-intensity optical field. The response is slightly different for a somewhat larger square-frame colloid (*i.e.* square), which has been designed to contain a central, square 2 μm x 2 μm hole. In the series of videos frames shown in Fig. 3 (Media 2), a square is initially held with its long-axes parallel to the focal plane with a $l = 6$ optical vortex. After the beam mode is switched to $l = 0$, the square translates to the left so that high-index SU-8 is within the high-intensity region of the optical trap and subsequently rotates 90° about $\mathbf{n}_0$ to an upright orientation. This rotation is reversible; after changing the beam mode back to $l = 6$ the square rotates back to its initial orientation with its long-axes parallel to the focal plane.

Due to the rotational symmetry about the optical axis of the intensity distribution of optical vortices, control over the sense of rotations about $\mathbf{n}_0$ induced by switching between various l's is somewhat limited. For example, in the series of video frames shown in Fig. 3, the triangle rotates 90° about $\mathbf{n}_0$ following a change of l from $l = 3$ to $l = 0$, then subsequently rotates a further 90° with the same sense when l is switched back to $l = 3$. However, depending on the precise initial conditions, the focal plane's vertical position with respect to the center of mass of the particle, and the particular sequence of vortex charges applied, one can rotate the triangle with either sense about $\mathbf{n}_0$ via changes of l.

#148001 - $15.00 USD Received 23 May 2011; revised 14 Jul 2011; accepted 10 Aug 2011; published 1 Sep 2011

Whether the particles are trapped upright with an $l = 0$ Gaussian trap or in-plane with a $l \neq 0$ optical vortex, they can be translated either by steering the trap within the field of view using computer-controlled holography or translating the sample using a stage. At the laser powers used in these studies (≤ 20 mW), the maximum velocities achievable before viscous drag forces pull the particle out of the trap are limited to ≈1-2 μm/s, because of the high shear viscosity of 5CB (η ~100 cP). Using a drag coefficient $\gamma \approx 2\text{x}10^{-6}$ kg/s determined in previous experiments [18] for similar square shaped colloids in 5CB, we estimate a maximum optical force without viscous drag pulling the particle out is ≈1-2 pN. Rotating the polarization of the beam parallel to $\mathbf{n}_0$ results in the colloid being pushed out of the trap for all shapes and any l, similar to the case of spherical colloids having refractive index intermediate between the ordinary and extraordinary indices of the LC which can be repelled or attracted to the laser trap by controlling beam's polarization [22]. Furthermore, in isotropic solvents, we cannot stably trap similar colloidal particles while keeping their long axes parallel to the focal plane for any l. This indicates that the restoring elastic torque provided by the NLC inhibits a tweezed particle from rotating about the optical axis due to angular momentum transfer, and stabilizes orientations dictated by the optical vortex that are not possible in isotropic liquids.

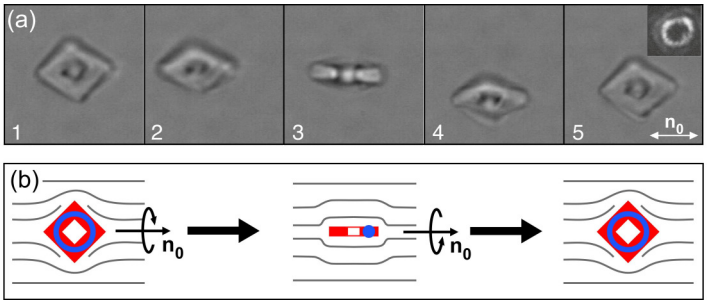

Fig. 3. (a) A series of frames taken from a video (Media 2) showing a square initially held with its long-axes parallel to the focal plane with a $l = 6$ vortex (inset). Switching the beam mode to $l = 0$ results in a ≈90° rotation and a translation to the left so that the square is standing upright with its high-index volume within the high-intensity region of the trap as shown in (b). Changing the beam mode back to $l = 6$ rotates the square back to its original orientation.

Using vortices having charge intermediate between $l = 0$ and $l = 6$ allows for fine control over the out of plane tilt of the square platelet, as shown in Fig. 4. The right hand side images show the stable equilibrium orientation of the square colloid trapped within optical vortices with charge $1 \leq l \leq 6$. As l increases, the tilt angle of the square continuously decreases from nearly 90° for $l = 1$ [Fig. 4(a)] to nearly zero for $l = 6$ [Fig. 4(f)]. In isotropic solvents, the radial component of the optical gradient force exerted by the Laguerre-Gaussian (LG) beams is known to trap high-index spherical colloids along the high-intensity ring in the lateral plane [4,11,12], and orbital angular momentum transferred from the beam can drive colloids around its circumference. However, in a planar NLC, elasticity suppresses rotations about the optical axis, and therefore, the plate-like colloid is constrained to rotate out of plane about an axis orthogonal to $\mathbf{n}_0$. We note that in samples with $\mathbf{n}_0$ perpendicular to the focal plane, a geometry for which the particle is free to rotate about the optical axis, plate-like colloids are attracted into the optical vortex and driven azimuthally around the ring presumably through orbital angular momentum transfer.

Shown on the left hand side of each panel in Fig. 4 are calculated intensity distributions within the focal plane (XY) and vertical cross-sections (XZ) over a 10 μm x 10 μm area. To obtain these distributions, we use the electric field amplitude E_p^l within the scalar wave approximation, which in cylindrical coordinates (r, φ, z) can be written

#148001 - $15.00 USD Received 23 May 2011; revised 14 Jul 2011; accepted 10 Aug 2011; published 1 Sep 2011

$$E_p^l \propto \exp\left[\frac{-ikr^2 z}{2\left(z_r^{\,2}+z^2\right)}\right]\exp\left[\frac{-r^2}{\omega^2}\right]\times$$
$$\exp\left[-i\left(2p+l+1\right)\arctan\left(z/z_r\right)\right]\exp\left[-il\varphi\right] \qquad (1)$$
$$\times\left(-1\right)^p\left(\frac{r\sqrt{2}}{\omega}\right)^l L_p^l\left(\frac{2r^2}{\omega^2}\right)$$

where l and p are mode indices, $k=2\pi n/\lambda \approx 8\times10^{-3}\text{nm}^{-1}$ is the wave number using a refractive index $n \approx 1.5$ and vacuum wavelength $\lambda = 1064$ nm, $\omega(z) = \omega_0[1 + (z/z_R)^2]^{1/2}$ is the beam waist at a distance z away from the focus along the optical axis, $z_r = \pi n\omega_0^2/\lambda$ is the Rayleigh length and $L_p^l(x)$ is a Laguerre-Gaussian polynomial [29].

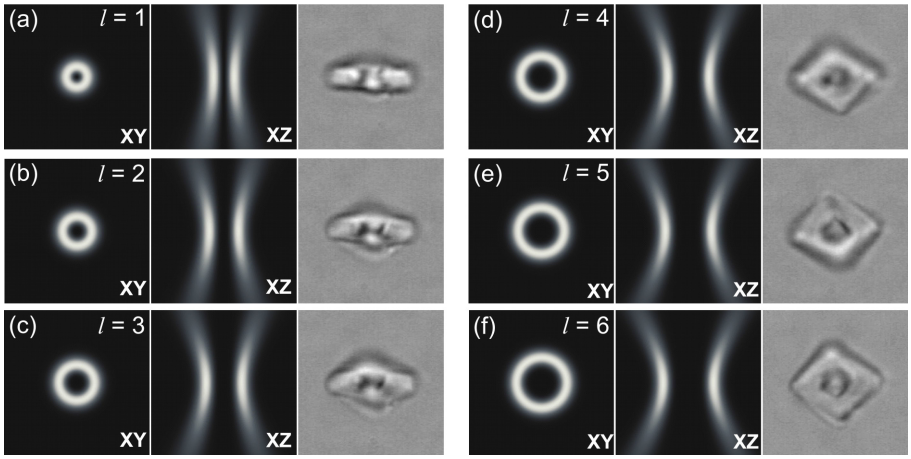

Fig. 4. Equilibrium orientations of a square colloid in 5CB as a function of vortex charge l and calculated three-dimensional intensity distributions of the optical vortices. The out of plane tilt angle of the square colloid decreases from (a) ≈90° at $l = 1$ to (f) ≈0° at $l = 6$ in order to maximize the volume of the high-index colloid within the highest intensity regions of the optical vortex. For all l, $p = 0$ and the beam waist at $z = 0$, $\omega_0 = 1$ μm.

Comparison of the observed equilibrium orientation of the square and the three-dimensional intensity profiles calculated using Eq. (1) indicate that the out of plane tilt of the square colloid is dictated predominately by maximizing the volume of the high index colloid within the high intensity regions of the trap. For example, since the lateral size of the LG beam in the XY-plane is smaller than or similar in size to the square hole within the colloid for $1 \le l \le 3$, the square must rotate out of plane to immerse a significant portion of its volume within the highest intensity regions of the vortex. Systematically less tilt is required as l is further increased above $l = 3$ until, at $l = 6$, no tilt is required. Thus, the tilt angle can be controlled continuously from 0° to 90° by adjusting the vortex charge l of the laser beam.

5. Conclusion

In conclusion, we have shown that holographic optical vortices can be utilized to optically trap and manipulate both the positions and orientations of complex-shaped colloidal particles through tuning the morphology of the optical field to the shape of the particle and suppressing the optical momentum transfer using an anisotropic host fluid. Since the rotational axis is collinear with the alignment direction of the NLC, which can be dynamically controlled using external fields, as is routinely accomplished in liquid crystal displays, a combination of optical vortex laser tweezers and external electric or magnetic fields may allow for full three dimensional orientational control. Although our studies have focused on lithographically fabricated SU-8 colloids suspended within a thermotropic nematic liquid crystal, we expect

#148001 - $15.00 USD Received 23 May 2011; revised 14 Jul 2011; accepted 10 Aug 2011; published 1 Sep 2011

that these strategies can be extended to other types and shapes of colloids as well as other anisotropic complex fluids such as surfactant or macromolecular based lyotropic liquid crystals, wormlike micellar fluids, and polymer solutions. Furthermore, employing other types of patterned optical fields such as modulated optical vortices [12], optical bottle beams [30], arrays of TEM_{00} mode traps [31], and line traps may allow for stable optical trapping, alignment, and rotation of colloidal particles with a variety of other complex morphologies.

Acknowledgments

We acknowledge the support of the Institute for Complex Adaptive Matter (ICAM) and the NSF grants no. DMR 0645461, DMR-0820579 and DMR-0847782 as well as the University of Colorado Innovation Seed Grant and Renewable Energy Initiative Seed Grant.

#148001 - $15.00 USD Received 23 May 2011; revised 14 Jul 2011; accepted 10 Aug 2011; published 1 Sep 2011